Flexibility in the Solution Structure of Human Tropoelastin†

Lisa D. Muiznieks and Anthony S. Weiss*

School of Molecular and Microbial Biosciences, The University of Sydney, Sydney, Australia 2006

Received January 23, 2007; Revised Manuscript Received April 26, 2007

ABSTRACT: We investigated the flexibility of full-length tropoelastin in solution by using far- and near-ultraviolet circular dichroism (UV CD) and fluorescence spectroscopy to probe for structural flexibility and residue mobility within secondary and tertiary features of the monomer. Fluorescence spectroscopy revealed the presence of exposed hydrophobicity through the binding of the hydrophobic probe 4,4′-dianilino-1,1′-binaphthyl-5,5′-disulfonate (bis-ANS), which demonstrates that hydrophobic regions form clusters and are not confined to a molecular core. Near-UV CD indicated substantial mobility of aromatic residues. Structural prediction programs (PONDR, DisEMBL, and Globplot version 2.0) estimated 75 ± 2% disorder in the tertiary structure of tropoelastin on the basis of primary sequence information. A single-site substitution of Trp for Gln (Q513W) at the tropoelastin domain 25−26 interface facilitated fluorescence spectroscopy for revealing that this region is exposed to solvent. Polarization anisotropy demonstrated substantial flexibility of W513 and little change upon denaturation of the monomer with guanidine hydrochloride. Comparable movement was found for native sequence aromatic residues in the presence of glycosaminoglycans and trifluoroethanol. These data prove the intrinsic flexibility of specific residues and adjacent sequences in any native conformation(s) they may take. This study is the first characterization of the level of mobility in defined regions of the full-length tropoelastin monomer and provides direct evidence for regions of flexible structure in tropoelastin.

Elastin provides repetitive elastic expansion and recoil to vertebrate tissues. The protein precursor tropoelastin is an extremely hydrophobic protein that self-associates and cross-links to form the mature elastic protein. Despite great effort, no single defined tertiary structure of tropoelastin has yet been defined. Secondary structural features of the monomer are far better understood than tertiary arrangement(s). Extensive documentation of secondary structural features of the full-length monomer of tropoelastin and peptide derivatives has been created using optical spectroscopies. Far-UV circular dichroism (CD), Fourier transform infrared (FT-IR), and Raman spectroscopy studies indicate tropoelastin contains a significant proportion (45−60%) of β-structure, including β-strand and turns, up to 40% random coil secondary structure, and little (3−10%) α-helix (*1*−*3*). Furthermore, the dominance of polyproline II structure in monomer tropoelastin and derivatives has been described (*4*−*6*) and is suggested to contribute to elasticity (*7*). This motif is characteristically short (approximately five residues) and does not contain hydrogen bonds, so it may exist transiently depending on the environmental solvent (*8*).

The sequence structure of tropoelastin is characterized by almost precisely alternating hydrophobic domains and cross-linking KA-rich domains, affording justification for the common reductionist approach to elastin structure and function investigation using elastin-like peptides as models of full-length tropoelastin. These constructs have taken a multitude of forms, including short synthetic sequence-derived peptides and repeats (*9*−*18*) and more recently whole domains, both in isolation (*4*−*6*, *19*−*22*) and in tandem combinations (*22*−*27*). NMR experiments provide evidence to show individual domains of tropoelastin, removed from the context of native sequence, are substantially unstructured and display a high degree of flexibility (*5*, *21*). Such domains transiently sample a variety of extended and closed conformational motifs, including loose polyproline II helix and some β-turn (*5*, *6*). Molecular dynamics simulations of the elastin-like polypeptide $(VPGVG)_{18}$ predict predominant disorder (*28*). These simulations describe hydrophobic domains as dynamic, with some distorted β-strand and fluctuating β-turns, and indicate the importance of a solvated protein environment for enabling conformational fluidity and facilitating elasticity.

No crystal structure of the full-length monomer is available; however, a small number of short elastin-derived peptides have been crystallized, including cyclic $(VPGVG)_3$ (*29*) and cyclic $(VPG)_4$ (*30*). These structures reveal the presence of type II β-turns. Likewise, NMR has yielded little to no tertiary structural resolution for the full-length tropoelastin monomer and, instead, points toward dynamic movement and substantial flexibility in the backbone peptide chain of mature cross-linked elastin and derivatives (*31*−*35*). Solid phase NMR studies of the elastin-like polypeptide $(LGGVG)_n$ ($n = 2-15$) reveal isolated β-turns located among substantial regions of disorder (*36*). These data show the polypeptide does not adopt a single conformation, inferring structural heterogeneity that may be representative of the native monomer.

† This work was supported by grants from the Australian Research Council and the University of Sydney to A.S.W. L.D.M. was a recipient of an Australian Postgraduate Research Scholarship.

* To whom correspondence should be addressed.

10.1021/bi700139k CCC: $37.00
Published on Web 06/14/2007

Analytical ultracentrifugation of the full-length tropoelastin monomer details the presence of at least two species in solution (*37*). Both are expanded asymmetrical shapes at physiological (37 °C) temperature, as measured by the calculation of frictional ratios greater than those expected for compact spherical conformations. The fitting of these sedimentation velocity data to two, in the simplest fit, separate but coexisting species raises several questions: (1) whether the monomer exists as a preferred (as few as two detectable conformations) subset of conformers or if it adopts a continuum of forms between the extended and globular dimensions defined by the ultracentrifugation studies and (2) if the monomer folds into defined, rigid structures or if conformers exhibit flexibility, either in individual domains or globally.

This work probed tertiary structural features of monomer human tropoelastin through an extensive study of structural motifs, including the clustering of hydrophobic residues, under various conditions relevant to the native extracellular matrix (ECM) environment of the monomer. Changes to structural features of the monomer were explored in the presence of heparin and chondroitin sulfate-B (CS-B) glycosaminoglycans (GAGs) and in the nonpolar solvent trifluoroethanol (TFE). Hydrophobic solvents provide an environment mimetic of that of the coacervate (*38*) and are well-known for inducing α-helix in proteins (*39*−*41*), including tropoelastin and derivatives (*6*, *38*, *42*), and for inducing expanded denatured states (*43*, *44*). Further, GAGs directly associate with elastic fibers in vivo (*45*, *46*). Thus, this system provided a representative model of structural features of tropoelastin examined in the native context of the full-length monomer.

A full-length tropoelastin mutant was created in which a glutamine residue at position 513 was replaced with a tryptophan residue to allow study of the structural features around this specific location, close to the protease hypersensitive border of domains 25 and 26 (*22*). We further extensively document the conformational stability of hydrophobic clusters and of aromatic residues and adjacent sequences within the context of the full-length tropoelastin monomer. The collection of studies presented here provides the most detailed description to date of structural features using the full-length monomer of human tropoelastin and illustrates substantial flexibility within the tertiary structure.

MATERIALS AND METHODS

Chemicals. Bis-ANS was obtained from Molecular Probes. 2,2,2-Trifluoroethanol, chondroitin sulfate-B sodium salt (porcine intestinal mucosa), and heparin sodium salt (porcine intestinal mucosa) were obtained from Sigma. All other reagents were analytical reagent grade.

Proteins. SHELΔ26A (tropoelastin) corresponds to a 60.1 kDa naturally occurring isoform of human tropoelastin lacking domain 26A. SHELΔ26A was prepared by overexpression in *Escherichia coli* BL21(DE3) cells and purified as previously described (*47*, *48*).

SHELΔ26A(Q513W) (hereafter called Q513W) corresponds to the 60.1 kDa SHELΔ26A isoform of tropoelastin with a single glutamine to tryptophan mutation at amino acid position 513. Q513W was constructed using the QuikChange site-directed mutagenesis kit (Stratagene). Oligonucleotide primers 5′-GTT GCT GCG AAA GCG TGG CTG CGT GCA GCA GCT G-3′ and 3′-CAG CTG CTG CAC GCA GCC ACG CTT TCG CAG CAA C-5′ were used to introduce the mutation into the template, pSHELΔ26A. Incorporation of the correct mutation was confirmed by DNA sequencing. The protein was prepared as previously described (*47*, *48*).

Fluorescence Spectroscopy. Fluorescence measurements were taken using a Cary Eclipse fluorescence spectrophotometer (Varian Inc.). Emission and excitation spectra were collected at wavelengths described in the figure legends using slit widths of 5 nm. Tryptophan and tyrosine residues were excited at 295 and 275 nm, respectively. Experiments were carried out in 10 mm fluorescence cuvettes. The cell temperature was controlled by an attached circulating water bath (Varian). Where required, bis-ANS (15 μM) was added to samples immediately prior to analysis and excited at 390 nm. For experiments that aimed to measure the effect of temperature on fluorescence emission intensity, samples were left to equilibrate for 5 min between changes in temperature.

Tropoelastin and Q513W were prepared to a concentration of 0.5 μM in either phosphate-buffered saline (PBS) or water before analysis of bound bis-ANS (in the case of tropoelastin) or intrinsic tryptophan fluorescence (in the case of Q513W). Where required, tropoelastin was treated in water with heparin or CS-B up to 17 μg/mL or with guanidine hydrochloride (GnHCl) or urea up to 5 M overnight at 37 °C. Quenching of tryptophan fluorescence in Q513W (0.5 μM) in PBS was carried out upon titration of acrylamide to 0.16 M at 37 °C. The collisional quenching constant K_{SV} was determined using the Stern−Volmer equation

$$F_0/F = 1 + K_{SV}[Q]$$

where F_0 and F are the intensities of sample fluorescence in the absence and presence of the quencher, respectively, and [Q] is the molar concentration of quencher (*49*).

The binding of bis-ANS to tropoelastin was analyzed by nonlinear regression using GraphPad Prism (version 4) from which an equilibrium dissociation constant (K_D) was derived.

Instrument voltage sensitivities were adjusted for each experiment with respect to protein concentration and the fluorophore signal intensity to obtain clear peak resolution and maxima where possible. The voltage was kept constant for traces depicted on the same set of axes in each case. All other instrument parameters and sample conditions were kept constant unless otherwise stated.

All spectra were corrected for variations in lamp intensity with emission wavelength using instrument correction curves. Traces were corrected for baseline buffer fluorescence, including Raman light scattering effects, and for changes in protein concentration introduced by sample dilution, where appropriate.

Circular Dichroism (CD) Spectropolarimetry. Far-UV CD spectra were obtained using a Jasco J-720 spectropolarimeter with a Neslab RTE-111 circulating water bath to control cell temperature. CD experiments were carried out in MQW at 37 °C unless otherwise stated using 0.2 mg/mL tropoelastin. Spectra were obtained using a 0.1 cm path length cell and collected between 184 and 260 nm. All CD experiments were conducted at a sensitivity of 20 mdeg with a 1.0 nm bandwidth and step resolution. All data are the average of

at least five accumulations and are expressed as molar ellipticity, [θ] (degrees square centimeters per decimole), according to the equation

$$[\theta] = (\text{ellipticity} \times \text{MRW})/[\text{cell path length (centimeters)} \times \text{concentration (milligrams per milliliter)} \times 10]$$

where the value used for mean residue weight (MRW) of both tropoelastin and Q513W was 86 Da. All traces were corrected for buffer and additive baselines as appropriate.

Secondary structure predictions were made using Varselec (*50*), which uses a variable selection method and a reference set of 33 proteins. Ellipticities were converted to $\Delta\epsilon$ by dividing by them 3300 (*51*) before Varselec analysis.

Near-UV CD was carried out as described above for far-UV CD, with the following changes. Tropoelastin was analyzed in PBS at 1.2 mg/mL in a 10 mm cuvette. Where required, TFE (to 5%), heparin (10 μg/mL), or CS-B (10 μg/mL) was added to tropoelastin in water, and spectra were recorded at 15 °C. Ribonuclease A was assayed as a control in water at a concentration of 2 mg/mL. Spectra were collected over the range of 250−320 nm.

Prediction of Intrinsically Disordered Sequence. The algorithms PONDR (*52*) (http://www.pondr.com/), DisEMBL (*53*), and GlobPlot 2 (*54*) (both at http://au.expasy.org/tools/) were used to predict regions of intrinsic tertiary structure disorder in the monomer of tropoelastin from the amino acid sequence. For each analysis, default program parameters were used.

Fluorescence Anisotropy. A manual polarizer accessory (Varian) was attached to a Cary Eclipse fluorescence spectrophotometer (Varian). Steady-state anisotropy (r) values were calculated as a ratio of the intensity (I) of vertically (v) and horizontally (h) polarized emission, according to the equation

$$r = I_{vv} - (GI_{vh})/I_{vv} + 2GI_{vh}$$

where G is the grating factor measured as I_{hv}/I_{hh} and the double subscripts refer to the direction of excitation and emission polarization, respectively (*55*).

Experiments were conducted at 25 °C using excitation and emission wavelengths of 295 and 350 nm for tryptophan, 280 and 325 nm for tyrosine, and 390 and 500 nm for bis-ANS, respectively. Slit widths of 10 nm were used. The protein concentration was kept constant at 0.5 μM in PBS. All other parameters were as described for fluorescence spectroscopy.

The rotational correlation time θ of the tropoelastin monomer was estimated as an indicator of whole protein movement (Brownian motion) of the monomer in solution using the equation

$$\theta = \eta M(\nu + h)/(RT)$$

where η is the solution viscosity, ν is partial specific volume, h is hydration, and M, R, and T are the molecular weight (daltons), universal gas constant (8.31×10^7 J K^{-1} mol^{-1}), and temperature (kelvin), respectively (*55*). In these experiments, the viscosity of PBS was taken as 0.01 P and the partial specific volume of tropoelastin monomer was taken to be 0.76 mL/g (*37*). A standard value of 0.23 g of water/g of protein was assumed for hydration (*55*).

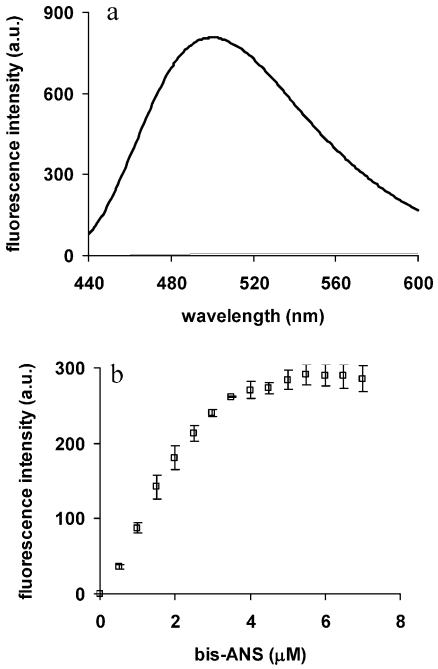

FIGURE 1: Binding of bis-ANS to tropoelastin. (a) Emission spectra of bis-ANS (15 μM) in PBS in the presence (thick) and absence (thin) of tropoelastin (0.5 μM). The fluorescence of tropoelastin (0.5 μM) in PBS alone is too low to be detected on this scale. Samples were excited at 390 nm and 37 °C. (b) Stoichiometry of binding of bis-ANS to tropoelastin. Titration of bis-ANS into tropoelastin (0.5 μM) in PBS at 37 °C. Fluorescence intensities are the average of three experiments and are reported ± the standard error of the mean.

RESULTS

Probing the Presence of Hydrophobic Clusters in Tropoelastin with Bis-ANS. Free probe in solution exhibited a fluorescence emission spectrum characterized by a peak around 535 nm when excited at 390 nm (Figure 1a). Interaction of the probe with tropoelastin was investigated by titration of the probe into a solution of tropoelastin (0.5 μM). Binding was saturable as demonstrated by a plateau in fluorescence intensity (Figure 1b). When binding became maximal, the fluorescence emission intensity of the probe significantly (greater than 100-fold) increased and the wavelength of maximal fluorescence emission was blue-shifted to approximately 495 nm (Figure 1a), demonstrating the presence of surface accessible hydrophobic clusters.

Analysis of Figure 1b revealed an approximate 10:1 binding stoichiometry of probe to tropoelastin monomer. This was further supported by the reverse titration of tropoelastin into bis-ANS (not shown). An average K_D of 0.35 ± 0.03 μM was estimated from the binding curves using GraphPad Prism (version 4).

Effect of Temperature on the Stability of Hydrophobic Clusters. When the temperature of the solution was incrementally increased from 15 to 50 °C, the fluorescence emission intensity of bound bis-ANS to tropoelastin decreased linearly by 30%, indicating disruption of monomer tertiary structure (Figure 2). The emission intensity exhibited complete reversibility when the sample was incrementally cooled to 15 °C.

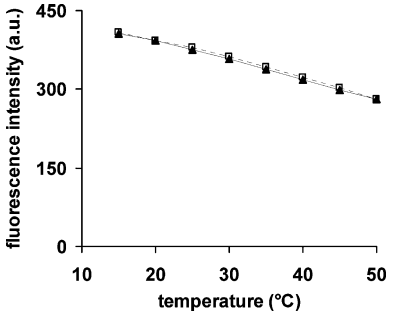

FIGURE 2: Effect of temperature on the clustering of hydrophobic residues of tropoelastin. A solution of tropoelastin (0.5 μM) and bis-ANS (15 μM) in water was incrementally heated (□, solid line) from 15 to 50 °C before the sample was cooled (▲, dashed line) to 15 °C. Fluorescence emission was collected at 492 nm upon excitation of the sample at 390 nm.

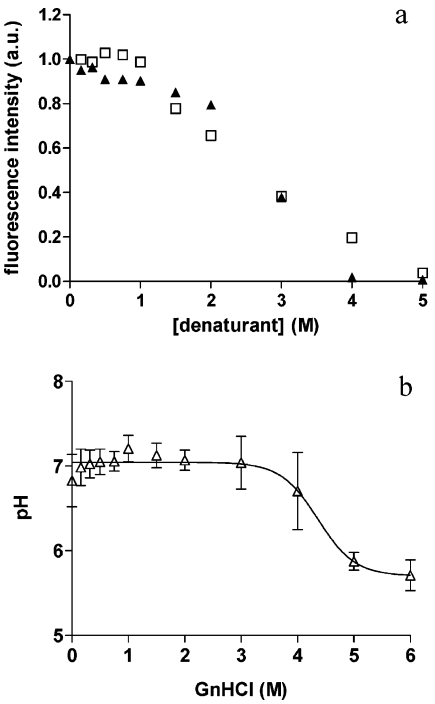

FIGURE 3: Effect of denaturants on the clustering of hydrophobic residues of tropoelastin. (a) The fluorescence emission intensity of bis-ANS (15 μM) bound to tropoelastin (0.5 μM) was measured upon titration with up to 5 M GnHCl (□) or urea (▲) in water at 37 °C. Fluorescence emission was collected at 495 nm upon excitation at 390 nm. (b) Change in the pH of tropoelastin and bis-ANS at 37 °C upon GnHCl titration.

Effect of Denaturants on the Stability of Hydrophobic Clusters. With up to 1 M GnHCl or urea, the emission intensity of bis-ANS remained relatively unchanged, indicating little disruption of tropoelastin structure under these conditions (Figure 3a). Further titration resulted in a steady decrease in fluorescence emission, which reached zero by the addition of 5 M denaturant, indicating complete disruption of bis-ANS binding.

The sample pH was measured upon titration of GnHCl to test the contribution of pH to the disruption of bis-ANS fluorescence. The pH of the solution remained constant with the addition of up to 3 M GnHCl (Figure 3b), by which concentration the fluorescence intensity of bis-ANS was 60% lower than in the absence of denaturants, as described above. Thus, the decrease in bis-ANS fluorescence emission intensity observed in these experiments was not a consequence of an induced pH change upon addition of denaturant.

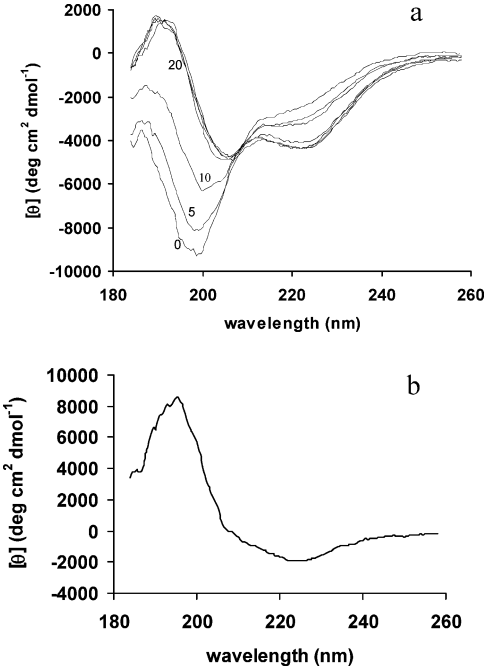

FIGURE 4: Effect of heparin on the secondary structure of tropoelastin. (a) CD spectra of tropoelastin (0.2 mg/mL) were collected in water with 5, 10, 20, 30, 40, and 50 μg/mL heparin. Traces with 20−50 μg/mL heparin overlay. (b). Difference spectrum between tropoelastin in the presence of 50 μg/mL heparin and water.

Effect of Glycosaminoglycans on Tropoelastin Structure. CD spectropolarimetry was used to measure secondary structural changes to monomer tropoelastin treated with heparin or CS-B. Titration of either GAG induced a red shift of the peak from 200 to 206 nm and a 1.6-fold increase in the intensity of the shoulder at 222 nm (Figures 4 and 5), characteristic of α-helix formation. The addition of heparin elicited a stronger structural effect at lower concentrations than CS-B. The maximum change with heparin was obtained by 20 μg/mL compared to the maximal response with CS-B at close to 80 μg/mL. An isodichroic point at 208 nm (heparin) and 212 nm (CS-B) revealed the structural change was probably due to a single secondary structure transition. This was supported using the Varselec program, which estimated that an increase to approximately 10% helix with heparin and CS-B was concomitant with a decrease in antiparallel β-sheet content.

The measured spectral shift may alternately indicate an increase in type I β-turn content (*56*). However, GAGs are strongly negatively charged and predicted to interact directly with tropoelastin through charges on lysine residues (*48*), compatible with the stabilization of nascent helix in alanine-rich sequence.

Effect of GAGs on the Stability of Hydrophobic Clusters. As expected from the substantial secondary structure change upon titration of GAGs, the tertiary conformation of the monomer shifted with addition of both heparin and CS-B. Bis-ANS binding sites were disrupted or shielded as measured by a decrease in bis-ANS fluorescence (Figure 6). Heparin was more effective than CS-B at effecting a change in fluorescence, reducing emission intensity to almost zero by the addition of 8 μg/mL. In contrast, disruption of bis-ANS fluorescence was initiated by CS-B at >4 μg/mL and

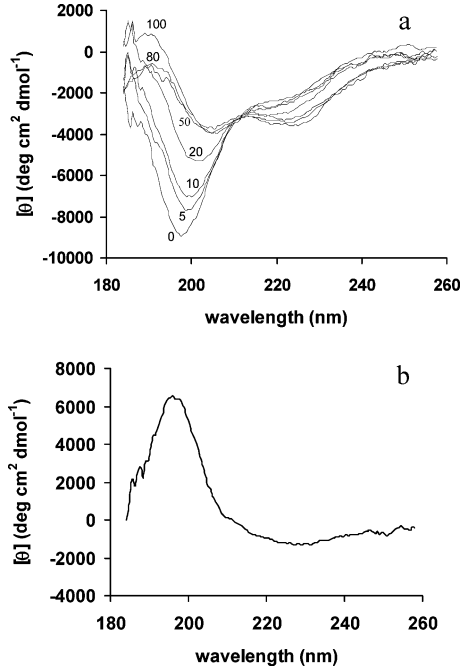

FIGURE 5: Effect of chondroitin sulfate B (CS-B) on the secondary structure of tropoelastin. (a) CD spectra of tropoelastin (0.2 mg/mL) were collected in water with 5, 10, 20, 50, 80, and 100 μg/mL CS-B. (b) Difference spectrum between tropoelastin in the presence of 100 μg/mL CS-B and water.

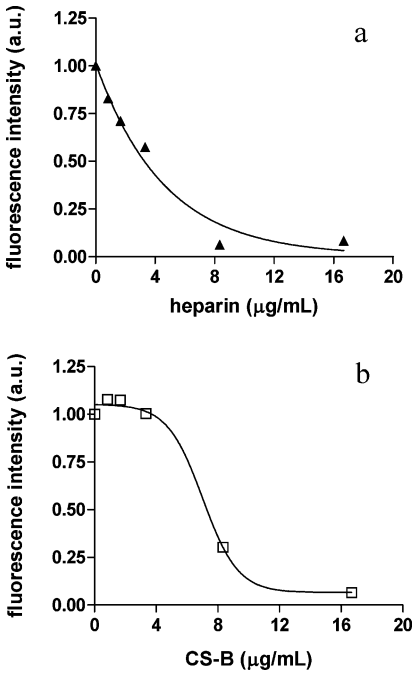

FIGURE 6: Effect of (a) heparin and (b) CS-B on the clustering of hydrophobic residues of tropoelastin. The fluorescence emission intensity of bis-ANS (15 μM) bound to tropoelastin (0.5 μM) in water was measured at 37 °C upon titration of GAGs. Fluorescence emission was collected at 495 nm upon excitation at 390 nm.

complete within the addition of 4-fold greater concentrations. These concentrations of GAGs were directly comparable to the GAGs:tropoelastin ratios required to induce α-helix formation.

Measuring the Secondary Structure Content of Q513W. The CD spectrum of Q513W, full-length tropoelastin in which glutamine 513 is replaced with tryptophan, overlaid the profile of native tropoelastin (Figure 7) and was

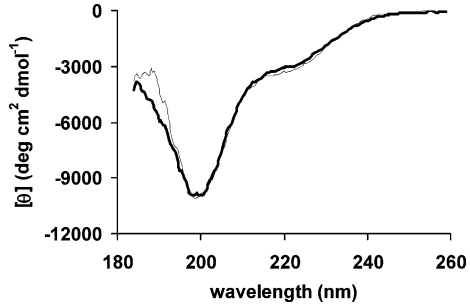

FIGURE 7: CD analysis of the glutamine 513 to tryptophan substitution. Circular dichroism trace of 0.2 mg/mL Q513W (thick) in water at 37 °C. The trace for tropoelastin (thin) obtained under the same conditions is shown for comparison.

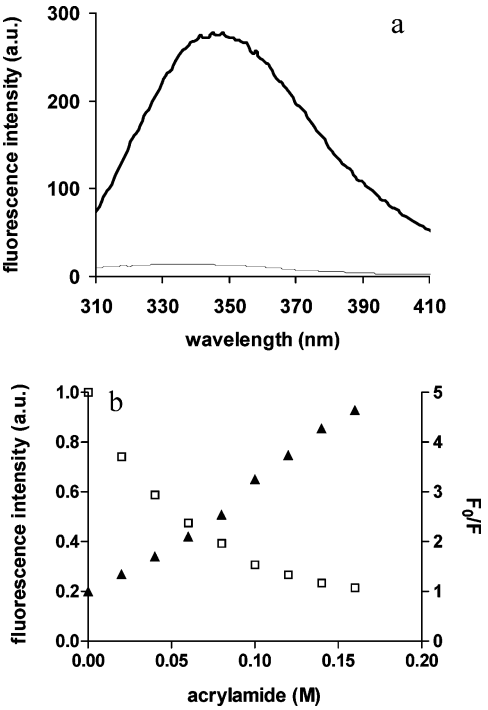

FIGURE 8: Monitoring the exposure of tryptophan 513 to solvent. (a) Fluorescence emission spectra of 0.5 μM Q513W (thick) or tropoelastin (thin) in PBS at 37 °C. Samples were excited at 295 nm. (b) Quenching of tryptophan 513 fluorescence emission with acrylamide (□) is shown with a Stern−Volmer plot (▲) of tryptophan 513 quenching.

characterized by a deep negative peak at 200 nm and a smaller negative shoulder at 220 nm. This indicated that the single glutamate to tryptophan substitution had little effect on the secondary structure of the construct compared to the native protein.

Monitoring the Fluorescence of Tryptophan 513. The emission spectrum of Q513W exhibited a fluorescence peak at 349 nm upon excitation of tryptophan at 295 nm, indicating the exposure of tryptophan to a polar solvent (Figure 8a). In comparison, the native tropoelastin monomer, containing no tryptophan residue, displayed minimal 295 and 349 nm excitation and emission fluorescence, respectively.

Acrylamide Quenching of Tryptophan 513. Titration of acrylamide to 0.16 M into a solution of Q513W decreased the intensity of tryptophan fluorescence emission by 80% (Figure 8b), indicating quenching of the tryptophan side chain, and resulted in a measured K_{SV} of 23.8 M^{-1}. This value is similar to the average value of 19.2 M^{-1} estimated

FIGURE 9: Prediction of disordered regions in tropoelastin from the amino acid sequence. Regions of predicted disorder are shown bold in uppercase. Results from three programs are shown aligned.

for iodide quenching of free tryptophan in solution (*57*), strongly indicating the highly solvent exposed location of tryptophan 513 in the tropoelastin construct here.

Prediction of Intrinsic Tertiary Structure Disorder in the Tropoelastin Monomer. Given the binding of the molten globule probe bis-ANS to full-length tropoelastin, tertiary structure disorder in the monomer was investigated using prediction programs. PONDR, GlobPlot, and DisEMBL estimated an average of 75 ± 1% disorder on the basis of analysis of the primary sequence (Figure 9). Although each program predicted a similar percentage of disorder, this was assigned to different regions of sequence, depending on the program that was used. GlobPlot and DisEMBL confined predictions of ordered tertiary structure to alanine-rich regions and localized disorder to hydrophobic domains. In contrast, PONDR predicted ordered and disordered regions that each contained hydrophobic and hydrophilic sequence. No obvious sequence features were identified to

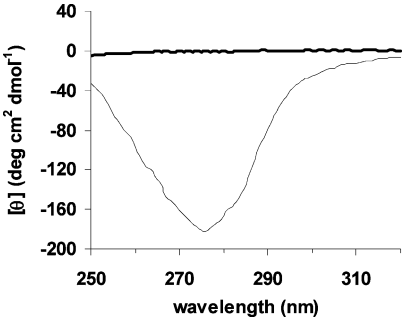

FIGURE 10: Near-UV CD of tropoelastin. The spectrum of tropoelastin (1.2 mg/mL) (thick) was collected in PBS at 37 °C. A control trace of ribonuclease A (2 mg/mL) (thin) was obtained in water at 37 °C.

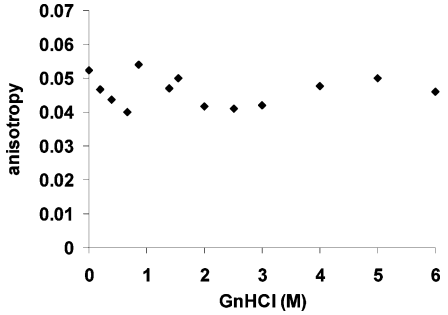

FIGURE 11: Effect of GnHCl on the fluorescence anisotropy of tryptophan. The fluorescence anisotropy of Q513W (0.5 μM) in PBS at 25 °C was measured in the absence of denaturant and upon titration of GnHCl to 6 M. W513 was excited at 295 nm, and emission was collected at 350 nm. All values are the average of eight readings.

account for the differences in structural predictions by the programs.

Mobility of the Conformational Environments of Aromatic Residues. Near-UV CD of tropoelastin revealed the absence of defined spectral peaks at 25 °C (Figure 10), indicating movement within the average local structural environments of aromatic (tyrosine and phenylalanine) residues. Increasing the tropoelastin concentration 1.67-fold to probe spectral definition did not alter the resolution of the trace. No change in the spectral profile was recorded at 15 °C or at temperatures of up to 65 °C measured in 10 °C increments. Furthermore, the addition of 5% TFE or of 10 μg/mL heparin or CS-B did not increase the tertiary structural definition of the tropoelastin monomer at 15 °C, as indicated by the lack of change in the near-UV CD spectrum compared to that for tropoelastin alone.

In contrast, the spectrum of ribonuclease A, taken here as a positive control, resembled the published spectrum (*58*). A strong negative peak was observed at 275 nm, indicative of the structurally rigid local environment around tyrosine residues (Figure 10).

Mobility of Aromatic Residues. The flexibility of tryptophan in the context of the full-length Q513W monomer was explored by steady-state fluorescence anisotropy. In PBS, the measured anisotropy of the indole ring was 0.05 $\pm$ 0.04. Relative to the limiting anisotropy (value for an immobile tryptophan) of approximately 0.27, as measured by Valeur and Weber (*59*) for tryptophan in propylene glycol at -50 °C, this indicates the flexibility of this tryptophan within the tropoelastin construct.

Titration of 6 M guanidine hydrochloride into a solution of Q513W was performed to relieve conformational restrictions imposed on the tryptophan residue. Concomitant measurement of steady-state anisotropy revealed no substantial effect of denaturation on the motional freedom of the indole ring, compared to that already permitted by the native conformation (Figure 11). This suggests little restriction of this tryptophan in the native conformational state.

The average flexibility of tyrosine residues in the tropoelastin monomer was investigated by steady-state anisotropy. The measured anisotropy of 0.07 $\pm$ 0.02 was substantially lower than the limiting steady-state anisotropy of 0.32, measured at -60 °C for *N*-acetyltyrosine amide in 70% propylene glycol (*60*), suggesting flexibility of the average tyrosine residue within the tropoelastin monomer.

Estimating Contributions to Fluorophore Depolarization from Whole Protein Diffusional Rotation. The rotational correlation time θ for the tropoelastin monomer was approximately 24 ns. Given the extended axial ratio (approximately 2) of the tropoelastin monomer (*37*), the actual value of θ may be up to twice as long (*55*). Compared to the relatively short (approximately 3 ns) average excited-state lifetimes of the intrinsic fluorophores used here (*60*, *61*), the substantially longer rotational correlation time suggests little contribution of whole monomer diffusion to residue depolarization. Therefore, the flexibility of residues measured here directly reflects the rotational motion of individual residues or the segmental motion of local sequence and is not due to the diffusional rotation of the whole monomer in solution.

Probing Segmental Flexibility within Tropoelastin. Anisotropy of bis-ANS bound to tropoelastin was explored to directly probe segmental motion within the tropoelastin monomer. Bis-ANS binds noncovalently, that is, through multiple attachment sites to accessible clusters of hydrophobic residues. Thus, the measured anisotropy of bound bis-ANS is reflective of the conformational plasticity of clustered pockets. The anisotropy of bound bis-ANS was 0.031 $\pm$ 0.003, measured upon saturation of tropoelastin with bis-ANS (greater than 10:1 probe to protein ratio), representing an average motional freedom of clustered hydrophobic regions within the tropoelastin monomer. This indicates the presence of substantial segmental flexibility within the tropoelastin monomer.

DISCUSSION

This work provides a description of tertiary structural features of the full-length tropoelastin monomer through the characterization of the surface accessibility and clustering of residues. By further targeting aromatic residues, we extended the study of structure to describe local conformational flexibility around these locations. Further direct indications of both residue and regional mobility within the native state of the full-length monomer were obtained by monitoring the average mobility of tryptophan and tyrosine residues by fluorescence anisotropy, and of hydrophobic clusters upon saturation of tropoelastin with bis-ANS.

Flexibility in the Tertiary Structure of Tropoelastin. The binding of bis-ANS to monomer tropoelastin under native environmental conditions allows for two main conclusions. First, the protein contains pockets of hydrophobic clusters.

Second, these clusters are solvent accessible, indicating that not all hydrophobic residues are confined to a molecular core.

Intrinsic consideration of folding restrictions preferentially confines hydrophobic domains and/or residues to a protein core, away from contact with polar solvent, leaving the presentation of hydrophilic residues at solvent−core interfaces. The abundance of hydrophobic residues in the primary sequence of tropoelastin led Gosline and colleagues (*62*) to demonstrate hydrophobic exposure (albeit limited) in mature elastin through the binding of ANS. The same study concomitantly postulated the solvent exposure of at least a subset of hydrophobic residues in the structure of the monomer. Recent demonstrations of the monomer existence of tropoelastin in solution in vitro below the critical concentration and temperature (*37*) and the absence of evidence of a molecular chaperone for the protein in the ECM support this suggestion.

Bis-ANS is fundamentally used to demonstrate the existence of molten globule states of proteins (*63*). Bis-ANS does not classically bind fully folded proteins due to the shielding of hydrophobic residues from the surrounding polar environment. Likewise, completely denatured proteins do not display local clusters of hydrophobicity and, thus, do not facilitate binding of the probe. While the binding of bis-ANS to tropoelastin shown here revealed the presence of at least isolated structure involving clustered hydrophobic residues, the solvent accessibility of these regions and the presence of substantial (45−60%) β-structure predominantly located within hydrophobic sequence (*1*−*3*) are consistent with the possibility of isolated molten globule structure(s).

These studies provide the first direct evidence of solvent accessibility of clustered hydrophobic residues in the monomer of tropoelastin. The average mobility within these clusters when bound by bis-ANS, as indicated by fluorescence anisotropy, and the computational prediction of 75% tertiary structural disorder predominantly within hydrophobic stretches directly corroborate these results. Moreover, the addition of GnHCl or urea completely denatures tertiary structure, as monitored by the disruption of hydrophobic clusters. However, as would be expected for a protein with independent clusters of structure, the unfolding transition is not sharp. In agreement with the structural dynamics inferred by these data, substantial flexibility of the peptide backbone of elastin has been documented well by NMR, including the mobility of up to 80% of backbone carbonyl carbons (*31*−*35*).

This report of intrinsic tertiary structural flexibility within the full-length monomer is in superb agreement with the dominant description of individual domains as conformational "ensembles" with regions of liquidlike dynamics (*5*, *6*, *12*, *20*, *64*). Furthermore, these data are compatible with the presence of the flexible and transient polyproline II motifs and more compact β-turns, while not precluding the presence of more defined structural motifs within regions of the sequence (*65*).

We show here the average tyrosine side chain is flexible using a combination of near-UV CD and fluorescence anisotropy. This is in agreement with the assertion that 12 of the 15 tyrosine residues in the monomer are likely to be exposed, as indicated by Raman spectroscopy (S. Mithieux, personal communication). Given the sequence location of six of these residues within or directly adjacent to hydrophilic stretches of alanine residues, long believed to be surface-exposed for cross-linking, the exposure of at least a subset of tyrosines is not surprising.

The flexibility of tertiary structure around these residues is sufficiently large to result in complete motional averaging, as monitored by near-UV CD. This technique is a reporter of the average movement of local conformational environments of aromatic residues. It is interesting to note that while ribonuclease exhibits a significantly weakened 275 nm tyrosine signal after denaturation when disulfide bonds are broken, the peak is not completely lost (*58*), which appears to be the case here for tropoelastin. Tropoelastin contains a lower percentage (2.1%) of tyrosine residues compared to ribonuclease (4.8%); however, the tropoelastin spectrum remained unchanged when the concentration was substantially increased. Further, results obtained using complementary optical techniques remain consistent with the existence of substantial tyrosine mobility in tropoelastin. Thus, taken together, these data corroborate structural flexibility around aromatic residues in the monomer. The alanine residues immediately adjacent to tyrosines in tropoelastin are presumably included in analysis of the structural setting around tyrosine residues, implying a concomitant degree of motion within these sequences. This structural instability is reflected in the existence of nascent α-helices in these alanine-rich regions (*42*).

Effect of GAGs, TFE, and Temperature on Monomer Flexibility. The decrease in bis-ANS fluorescence upon addition of GAGs indicates the disruption of hydrophobic clusters or their shielding from solvent. As GAGs are known to interact directly with the tropoelastin monomer (*48*, *66*), this may suggest shielding of residues. Given the likely induction of α-helical secondary structure in the tropoelastin monomer by GAGs described here, it is possible they concomitantly stabilize the tertiary conformation. However, the lack of changes to the near-UV CD profile upon addition of GAGs suggests that, at least at low concentrations, binding does not measurably induce formation of a more stable monomer tertiary structure. An analogous conclusion can be drawn for tropoelastin in the presence of TFE.

Similarly, the decrease in the level of bis-ANS binding to tropoelastin with an increase in temperature indicates there are fewer accessible hydrophobic clusters in the monomer. This may be due to disruption of hydrophobic clusters or the decrease in their solvent accessibility, possibly by residue shielding. Far-UV CD of full-length monomer tropoelastin reveals a slight increase in β-structure content with temperature (N. Sue and A. Weiss, personal communication). Disruption due to shielding by other monomers is unlikely given the absence of coacervation under the conditions of low protein concentration and the lack of salt used here. However, an increasing temperature did not concomitantly increase the spectral definition of the near-UV CD profile. Although the spectral resolution is low, these data indicate the application of temperature may not increase order within the tertiary structure of the monomer. Therefore, although secondary structure may be affected upon binding of tropoelastin to elastic fiber proteins or with an increase in temperature, tertiary conformational confinement of the monomer may well remain relatively weak.

The global conformational plasticity of the monomer was not measurably affected upon binding to the GAGs heparin

and CS-B or in the highly nonpolar solvent TFE. Specific investigation of structural features of tropoelastin bound to elastic fiber proteins is likely to further indicate whether the intrinsic conformational flexibility of the monomer is retained in the context of mature elastin. Indeed, backbone flexibility is retained even in mature elastin, as demonstrated using native elastin fibers (*33*).

Thus, the current data allow for a detailed description of structural features of tropoelastin in the context of the full-length monomer. These data suggest that the solvent exposure of multiple clusters of hydrophobic resides is a natural consequence of the high hydrophobic sequence content of the protein. The tryptophan residue located close to the border of domains 25 and 26 and tyrosine residues exhibited movement within the content of the full-length sequence. Additionally, the conformational environments around aromatic residues were identified as flexible. This dynamic structural characterization supports the fluctuation of sequence within a loose net of extended dimensions, as reported for the monomer in solution at 37 °C (*37*), where flexibility within the tertiary structure of tropoelastin, and the likely consequence of a continuum of forms, does not affect incorporation of conformers into the coacervate (*37*). This further remains consistent with the substantial flexibility of the mature elastin backbone (*32*−*34*) and the primary elastic function of the protein.

ACKNOWLEDGMENT

We gratefully acknowledge the construction of Q513W by A. Maxwell and the production of SHELΔ26A by O. Regaglia and K. Schultz. We appreciate generous advice from Drs. R. Clarke and W. Sawyer on fluorescence techniques.

REFERENCES

1. Debelle, L., Alix, A. J., Jacob, M. P., Huvenne, J. P., Berjot, M., Sombret, B., and Legrand, P. (1995) Bovine elastin and κ-elastin secondary structure determination by optical spectroscopies, *J. Biol. Chem. 270*, 26099−26103.
2. Vrhovski, B., Jensen, S., and Weiss, A. S. (1997) Coacervation characteristics of recombinant human tropoelastin, *Eur. J. Biochem. 250*, 92−98.
3. Debelle, L., and Alix, A. J. P. (1995) Optical spectroscopic determination of bovine tropoelastin molecular model, *J. Mol. Struct. 348*, 321−324.
4. Bochicchio, B., Ait-Ali, A., Tamburro, A. M., and Alix, A. J. (2004) Spectroscopic evidence revealing polyproline II structure in hydrophobic, putatively elastomeric sequences encoded by specific exons of human tropoelastin, *Biopolymers 73*, 484−493.
5. Bochicchio, B., Floquet, N., Pepe, A., Alix, A. J., and Tamburro, A. M. (2004) Dissection of human tropoelastin: Solution structure, dynamics and self-assembly of the exon 5 peptide, *Chem.*−*Eur. J. 10*, 3166−3176.
6. Tamburro, A. M., Bochicchio, B., and Pepe, A. (2003) Dissection of human tropoelastin: Exon-by-exon chemical synthesis and related conformational studies, *Biochemistry 42*, 13347−13362.
7. Martino, M., Bavoso, A., Guantieri, V., Coviello, A., and Tamburro, A. M. (2000) On the occurence of polyproline II structure in elastin, *J. Mol. Struct. 519*, 173−189.
8. Bochicchio, B., and Tamburro, A. M. (2002) Polyproline II structure in proteins: Identification by chiroptical spectroscopies, stability, and functions, *Chirality 14*, 782−792.
9. Broch, H., Moulabbi, M., Vasilescu, D., and Tamburro, A. M. (1996) Conformational and electrostatic properties of V-G-G-V-G, a typical sequence of the glycine-rich regions of elastin. An ab initio quantum molecular study, *Int. J. Pept. Protein Res. 47*, 394−404.
10. Broch, H., Moulabbi, M., Vasilescu, D., and Tamburro, A. M. (1998) Quantum molecular modeling of the elastinic tetrapeptide Val-Pro-Gly-Gly, *J. Biomol. Struct. Dyn. 15*, 1073−1091.
11. Castiglione-Morelli, A., Scopa, A., Tamburro, A. M., and Guantieri, V. (1990) Spectroscopic studies on elastin-like synthetic polypeptides, *Int. J. Biol. Macromol. 12*, 363−368.
12. Floquet, N., Hery-Huynh, S., Dauchez, M., Derreumaux, P., Tamburro, A. M., and Alix, A. J. (2004) Structural characterization of VGVAPG, an elastin-derived peptide, *Biopolymers 76*, 266−280.
13. Tamburro, A. M., Guantieri, V., and Gordini, D. D. (1992) Synthesis and structural studies of a pentapeptide sequence of elastin. Poly(Val-Gly-Gly-Leu-Gly), *J. Biomol. Struct. Dyn. 10*, 441−454.
14. Rapaka, R. S., and Urry, D. W. (1978) Coacervation of sequential polypeptides models of tropoelastin. Synthesis of H-(Val-Ala-Pro-Gly)$_n$-Val-OMe and H-(Val-Pro-Gly-Gly)$_n$-Val-OMe, *Int. J. Pept. Protein Res. 11*, 97−108.
15. Thomas, G. J., Jr., Prescott, B., and Urry, D. W. (1987) Raman amide bands of type-II β-turns in cyclo-(VPGVG)$_3$ and poly-(VPGVG), and implications for protein secondary-structure analysis, *Biopolymers 26*, 921−934.
16. Urry, D. W., Long, M. M., Ohnishi, T., and Jacobs, M. (1974) Circular dichroism and absorption of the polytetrapeptide of elastin: A polymer model for the β-turn, *Biochem. Biophys. Res. Commun. 61*, 1427−1433.
17. Urry, D. W., Mitchell, L. W., Ohnishi, T., and Long, M. M. (1975) Proton and carbon magnetic resonance studies of the synthetic polypentapeptide of elastin, *J. Mol. Biol. 96*, 101−117.
18. Urry, D. W., Onishi, T., Long, M. M., and Mitchell, L. W. (1975) Studies on the conformation and interactions of elastin: Nuclear magnetic resonance of the polyhexapeptide, *Int. J. Pept. Protein Res. 7*, 367−378.
19. Floquet, N., Pepe, A., Dauchez, M., Bochicchio, B., Tamburro, A. M., and Alix, A. J. (2005) Structure and modeling studies of the carboxy-terminus region of human tropoelastin, *Matrix Biol. 24*, 271−282.
20. Pepe, A., Guerra, D., Bochicchio, B., Quaglino, D., Gheduzzi, D., Pasquali Ronchetti, I., and Tamburro, A. M. (2005) Dissection of human tropoelastin: Supramolecular organization of polypeptide sequences coded by particular exons, *Matrix Biol. 24*, 96−109.
21. Mackay, J. P., Muiznieks, L. D., Toonkool, P., and Weiss, A. S. (2005) The hydrophobic domain 26 of human tropoelastin is unstructured in solution, *J. Struct. Biol. 150*, 154−162.
22. Jensen, S. A., Vrhovski, B., and Weiss, A. S. (2000) Domain 26 of tropoelastin plays a dominant role in association by coacervation, *J. Biol. Chem. 275*, 28449−28454.
23. Bellingham, C. M., Woodhouse, K. A., Robson, P., Rothstein, S. J., and Keeley, F. W. (2001) Self-aggregation characteristics of recombinantly expressed human elastin polypeptides, *Biochim. Biophys. Acta 1550*, 6−19.
24. Miao, M., Bellingham, C. M., Stahl, R. J., Sitarz, E. E., Lane, C. J., and Keeley, F. W. (2003) Sequence and Structure Determinants for the Self-aggregation of Recombinant Polypeptides Modeled after Human Elastin, *J. Biol. Chem. 278*, 48553−48562.
25. Miao, M., Cirulis, J. T., Lee, S., and Keeley, F. W. (2005) Structural determinants of cross-linking and hydrophobic domains for self-assembly of elastin-like polypeptides, *Biochemistry 44*, 14367−14375.
26. Rodgers, U. R., and Weiss, A. S. (2004) Integrin avb3 binds a unique non-RGD site near the C-terminus of human tropoelastin, *Biochimie 86*, 173−178.
27. Toonkool, P., Jensen, S. A., Maxwell, A. L., and Weiss, A. S. (2001) Hydrophobic domains of human tropoelastin interact in a context-dependent manner, *J. Biol. Chem. 276*, 44575−44580.
28. Li, B., and Daggett, V. (2002) Molecular basis for the extensibility of elastin, *J. Muscle Res. Cell Motil. 23*, 561−573.
29. Cook, W. J., Einspahr, H., Trapane, T. L., Urry, D. W., and Bugg, C. E. (1980) Crystal structure and conformation of the cyclic trimer of a repeat pentapeptide of elastin, cyclo-(L-valyl-L-prolylglycyl-L-valylglycyl)$_3$, *J. Am. Chem. Soc. 102*, 5502−5505.
30. Cook, W. J., Trapane, T. L., and Prasad, K. U. (1985) Crystal structure and conformation of the cyclic tetramer of a repeat tripeptide of elastin, cyclo(L-valyl-L-prolylglycyl)$_4$, *Int. J. Pept. Protein Res. 25*, 481−486.
31. Torchia, D. A., and Sullivan, C. E. (1977) A ^{13}C magnetic resonance study of embryonic chick aorta, *Adv. Exp. Med. Biol. 79*, 655−661.

32. Lyerla, J. R., Jr., and Torchia, D. A. (1975) Molecular mobility and structure of elastin deduced from the solvent and temperature dependence of ^{13}C magnetic resonance relaxation data, *Biochemistry 14*, 5175−5183.
33. Pometun, M. S., Chekmenev, E. Y., and Wittebort, R. J. (2004) Quantitative observation of backbone disorder in native elastin, *J. Biol. Chem. 279*, 7982−7987.
34. Perry, A., Stypa, M. P., Foster, J. A., and Kumashiro, K. K. (2002) Observation of the glycines in elastin using ^{13}C and ^{15}N solid-state NMR spectroscopy and isotopoc labeling, *J. Am. Chem. Soc. 124*, 6832−6833.
35. Torchia, D. A., and Piez, K. A. (1973) Mobility of elastin chains as determined by ^{13}C nuclear magnetic resonance, *J. Mol. Biol. 76*, 419−424.
36. Kumashiro, K. K., Kurano, T. L., Niemczura, W. P., Martino, M., and Tamburro, A. M. (2003) ^{13}C CPMAS NMR studies of the elastin-like polypeptide $(LGGVG)_n$, *Biopolymers 70*, 221−226.
37. Toonkool, P., Regan, D. G., Kuchel, P. W., Morris, M. B., and Weiss, A. S. (2001) Thermodynamic and hydrodynamic properties of human tropoelastin. Analytical ultracentrifuge and pulsed field-gradient spin-echo NMR studies, *J. Biol. Chem. 276*, 28042−28050.
38. Starcher, B. C., Saccomani, G., and Urry, D. W. (1973) Coacervation and ion-binding studies on aortic elastin, *Biochim. Biophys. Acta 310*, 481−486.
39. Hirota, N., Mizuno, K., and Goto, Y. (1998) Group additive contributions to the alcohol-induced α-helix formation of melittin: Implication for the mechanism of the alcohol effects on proteins, *J. Mol. Biol. 275*, 365−378.
40. Hirota, N., Mizuno, K., and Goto, Y. (1997) Cooperative α-helix formation of *β*-lactoglobulin and melittin induced by hexafluoroisopropanol, *Protein Sci. 6*, 416−421.
41. Reiersen, H., and Rees, A. R. (2000) Trifluoroethanol may form a solvent matrix for assisted hydrophobic interactions between peptide side chains, *Protein Eng. 13*, 739−743.
42. Muiznieks, L. D., Jensen, S. A., and Weiss, A. S. (2003) Structural changes and facilitated association of tropoelastin, *Arch. Biochem. Biopyhs. 410*, 317−323.
43. Kamatari, Y. O., Konno, T., Kataoka, M., and Akasaka, K. (1996) The methanol-induced globular and expanded denatured states of cytochrome c: A study by CD fluorescence, NMR and small-angle X-ray scattering, *J. Mol. Biol. 259*, 512−523.
44. Kamatari, Y. O., Ohji, S., Konno, T., Seki, Y., Soda, K., Kataoka, M., and Akasaka, K. (1999) The compact and expanded denatured conformations of apomyoglobin in the methanol-water solvent, *Protein Sci. 8*, 873−882.
45. Gheduzzi, D., Guerra, D., Bochicchio, B., Pepe, A., Tamburro, A. M., Quaglino, D., Mithieux, S., Weiss, A. S., and Pasquali Ronchetti, I. (2005) Heparan sulphate interacts with tropoelastin, with some tropoelastin peptides and is present in human dermis elastic fibers, *Matrix Biol. 24*, 15−25.
46. Fornieri, C., Baccarani-Contri, M., Quaglino, D., Jr., and Pasquali-Ronchetti, I. (1987) Lysyl oxidase activity and elastin/glycosaminoglycan interactions in growing chick and rat aortas, *J. Cell Biol. 105*, 1463−1469.
47. Martin, S. L., Vrhovski, B., and Weiss, A. S. (1995) Total synthesis and expression in *Escherichia coli* of a gene encoding human tropoelastin, *Gene 154*, 159−166.
48. Wu, W. J., Vrhovski, B., and Weiss, A. S. (1999) Glycosaminoglycans mediate the coacervation of human tropoelastin through dominant charge interactions involving lysine side chains, *J. Biol. Chem. 274*, 21719−21724.
49. Eftink, M. R., and Ghiron, C. A. (1981) Fluorescence quenching studies with proteins, *Anal. Biochem. 114*, 199−227.
50. Manavalan, P., and Johnson, W. C., Jr. (1987) Variable selection method improves the prediction of protein secondary structure from circular dichroism spectra, *Anal. Biochem. 167*, 76−85.
51. Strickland, E. H. (1974) Aromatic contributions to circular dichroism spectra of proteins, *CRC Crit. Rev. Biochem. 2*, 113−175.
52. Romero, P. Z., Obradovic, Z., Kissinger, C. R., Villafranca, J. E., and Dunker, A. K. (1997) Identifying Disordered Regions in Proteins from Amino Acid Sequences, *Proc.-IEEE Int. Conf. Neural Networks 1*, 90−95.
53. Linding, R., Jensen, L. J., Diella, F., Bork, P., Gibson, T. J., and Russell, R. B. (2003) Protein disorder prediction: Implications for structural proteomics, *Structure 11*, 1453−1459.
54. Linding, R., Russell, R. B., Neduva, V., and Gibson, T. J. (2003) GlobPlot: Exploring protein sequences for globularity and disorder, *Nucleic Acids Res. 31*, 3701−3708.
55. Lakowicz, J. R. (1999) *Principles of fluorescence spectroscopy*, Kluwer Academic/Plenum Publishers, New York.
56. Perczel, A., and Fasman, G. D. (1992) Quantitative analysis of cyclic *β*-turn models, *Protein Sci. 1*, 378−395.
57. Louzada, P. R., Sebollela, A., Scaramello, M. E., and Ferreira, S. T. (2003) Predissociated dimers and molten globule monomers in the equilibrium unfolding of yeast glutathione reductase, *Biophys. J. 85*, 3255−3261.
58. Tamburro, A. M., Boccu, E., and Celotti, L. (1970) The role of disulfide bonds in the protein structure. Conformational studies on reduced ribonuclease and lysozyme, *Int. J. Protein Res. 2*, 157−164.
59. Valeur, B., and Weber, G. (1977) Resolution of the fluorescence excitation spectrum of indole into the 1La and 1Lb excitation bands, *Photochem. Photobiol. 25*, 441−444.
60. Gryczynski, I., Steiner, R. F., and Lakowicz, J. R. (1991) Intensity and anisotropy decays of the tyrosine calmodulin proteolytic fragments, as studied by GHz frequency-domain fluorescence, *Biophys. Chem. 39*, 69−78.
61. Ferreira, S. T. (1989) Fluorescence studies of the conformational dynamics of parvalbumin in solution: Lifetime and rotational motions of the single tryptophan residue, *Biochemistry 28*, 10066−10072.
62. Gosline, J. M., Yew, F. F., and Weis-Fogh, T. (1975) Reversible structural changes in a hydrophobic protein, elastin, as indicated by fluorescence probe analysis, *Biopolymers 14*, 1811−1826.
63. Chapeaurouge, A., Johansson, J. S., and Ferreira, S. T. (2002) Folding of a de novo designed native-like four-helix bundle protein, *J. Biol. Chem. 277*, 16478−16483.
64. Tamburro, A. M., Bochicchio, B., and Pepe, A. (2005) The dissection of human tropoelastin: From the molecular structure to the self-assembly to the elasticity mechanism, *Pathol. Biol. 53*, 383−389.
65. Tamburro, A. M., Pepe, A., and Bochicchio, B. (2006) Localizing α-helices in human tropoelastin: Assembly of the elastin "puzzle", *Biochemistry 45*, 9518−9530.
66. Broekelmann, T. J., Kozel, B. A., Ishibashi, H., Werneck, C. C., Keeley, F. W., Zhang, L., and Mecham, R. P. (2005) Tropoelastin interacts with cell-surface glycosaminoglycans via its COOH-terminal domain, *J. Biol. Chem. 280*, 40939−40947.

BI700139K